

Advances in boronization on NSTX-Upgrade



C. H Skinner^{a,*}, F. Bedoya^b, F. Scotti^c, J.P. Allain^b, W. Blanchard^a, D. Cai^a, M. Jaworski^a, B.E. Koel^d

^a Princeton Plasma Physics Laboratory, Princeton, NJ 08543 USA

^b Department of Nuclear, Plasma, and Radiological Engineering, University of Illinois, Urbana, IL 61801, USA

^c Lawrence Livermore National Laboratory, Livermore, CA 94550, USA

^d Department of Chemical and Biological Engineering, Princeton University, Princeton, NJ 08540, USA

ARTICLE INFO

Article history:

Received 13 July 2016

Revised 11 November 2016

Accepted 26 November 2016

Available online 27 January 2017

Keywords:

Boronization

Deuterated tri-methyl boron

NSTX-U

Plasma-materials interaction

Surface analysis

ABSTRACT

Boronization has been effective in reducing plasma impurities and enabling access to higher density, higher confinement plasmas in many magnetic fusion devices. The National Spherical Torus eXperiment, NSTX, has recently undergone a major upgrade to NSTX-U in order to develop the physics basis for a ST-based Fusion Nuclear Science Facility (FNSF) with capability for double the toroidal field, plasma current, and NBI heating power and increased pulse duration from 1–1.5 s to 5–8 s. A new deuterated tri-methyl boron conditioning system was implemented together with a novel surface analysis diagnostic. We report on the spatial distribution of the boron deposition versus discharge pressure, gas injection and electrode location. The oxygen concentration of the plasma facing surface was measured by in-vacuo XPS and increased both with plasma exposure and with exposure to trace residual gases. This increase correlated with the rise of oxygen emission from the plasma.

© 2016 Elsevier Ltd.

This is an open access article under the CC BY-NC-ND license.

(<http://creativecommons.org/licenses/by-nc-nd/4.0/>)

1. Introduction

The composition of the plasma facing surface has a profound effect on plasma performance, as most recently evidenced by the results from the JET-ILW [1]. The reservoir of particles in the wall surface that are accessible by sputtering typically exceeds the plasma particle content by orders-of-magnitude and hydrogenic and impurity influx needs to be controlled to permit density control and to minimize radiative losses. Wall conditioning has proved to be key to obtaining high plasma performance [2] and one of the most successful techniques is plasma assisted chemical vapor deposition of boron on plasma facing surfaces as reviewed in ref. [3]. This technique was pioneered at TEXTOR [4] using a radiofrequency assisted glow discharge of 80% He, 10% CH₄ and 10% diborane (B₂H₆) that deposited a 40 nm thick amorphous boron/carbon film (a-B/C:D). This film gettered oxygen, resisted chemical erosion and led to tokamak discharges with significantly reduced oxygen and carbon impurities. Diborane needs special handling due to its explosive and toxic properties, however boronization using the less hazardous compound, trimethyl boron, B(CH₃)₃ was found to have similar effects [5]. Boronization was originally applied

to the National Spherical Torus eXperiment (NSTX) using a glow discharge with 90% helium and 10% deuterated trimethyl boron (dTMB) [6] and after 2004, a 95% helium and 5% dTMB mixture. dTMB is used as hydrogen is incompatible with High Harmonic Fast Wave heating due to parasitic resonances. This boronization was successful in increasing the current flat-top time by 70%, reducing radiated power by a factor of 2, reducing Z_{eff} by a factor of 3, reducing oxygen impurity brightness by a factor of 15 and reducing copper impurities to below the detection threshold. These changes enabled access to higher density, higher confinement plasmas, including H mode conditions.

The deposition of boron is intimately related to the physics of the associated plasma. Glow discharges (GDC) were first developed in the 19th century and have been widely used to clean and condition the vessel walls in fusion devices. They are low-temperature plasma discharges, between one or more anodes inserted into the tokamak vessel and the vessel wall serving as a cathode. The physics of glow discharges came under investigation recently as they will be one of the primary conditioning techniques used in ITER [7,8]. Of primary interest is the ion current density impacting the wall component surfaces, which must be as uniform as possible. An important insight reported in [7] is that the GDC discharge operates basically as a hollow-cathode discharge: the plasma is sustained mainly by ionization by secondary elec-

* Corresponding author.

E-mail address: cskinner@pppl.gov (C.H. Skinner).

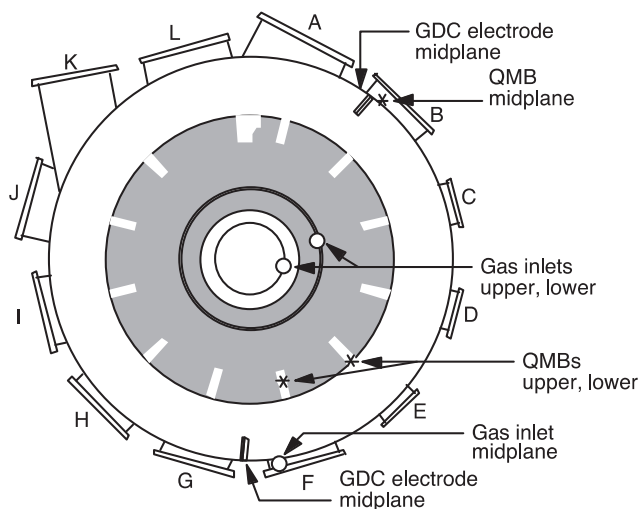


Fig. 1. Top view of the NSTX-U vessel with location of the GDC electrodes, dTMB gas inlet, and QMBs. The grey area indicates the inner and outer divertor. The major radius of the vessel wall is 1.7 m. (For interpretation of the references to colour in this figure legend, the reader is referred to the web version of this article.)

trons emitted from the cathode, accelerated ballistically through a thin cathode sheath, penetrating the plasma as a fast electron beam, and trapped by the cathode fall surrounding the plasma on all sides. The anode has a much lower surface area compared to the cathode (vessel wall) and this leads to the formation of an anode glow and an order-of-magnitude higher ion flux in the vicinity of the anode.

Chemical characterization of boron on graphite samples and the interactions of boron deposits with a plasma were investigated on RFX [9,10]. The boron deposition was enhanced in the vicinity of the glow discharge anode as expected and oxygen at a 5% level was found in the deposited layer. This increased to 10% after plasma exposure and reduced the capacity for hydrogen gettering over time.

2. Boronization system on NSTX-U

NSTX has recently undergone a major upgrade to NSTX-U in order to develop the physics basis for a ST-based Fusion Nuclear Science Facility (FNSF) [11] by exploring low collisionality regimes. NSTX-U will double the toroidal field, plasma current, and NBI heating power and increase the pulse duration from 1–1.5 s to 5–8 s. At present, typical NSTX-U discharges are ~1 s duration and operate every 17.5 min with a 8 min period of He-GDC between discharges. H-mode was accessed during the first two weeks of operations after the first boronization was performed and Neutral Beam Injection (NBI) used to heat the plasma [12]. The NSTX-U vacuum vessel comprises 12 bays labelled A–L, see Fig. 1. The previous boronization system on NSTX had just one injection point on the midplane (Bay L) and experienced highly non-uniform boron deposition - quartz microbalance measurements showed 25–47× less boron deposited on the lower and upper divertor than on the midplane. A new deuterated trimethylboron (dTMB) system [13] has been installed on NSTX-U that injects a 5% dTMB/ 95% helium mix from any of three gas inlet ports (Bay C lower, Bay F midplane and Bay D center column top) during a glow discharge. The system has five major sub-assemblies: (i) helium control panel, (ii) dTMB cabinet, (iii) mass flow controller box, (iv) coaxial injection lines and (v) vacuum pumping assemblies. Safety features include a 6" diameter 5.7 standard m³/min exhaust of the dTMB gas cabinet, dTMB gas detection at ppm level and an internal fire sprinkler with a fuse rating of 68 °C. The gas is delivered to the NSTX-U vessel via a 6 mm i.d. process gas line inside a 13 mm contain-

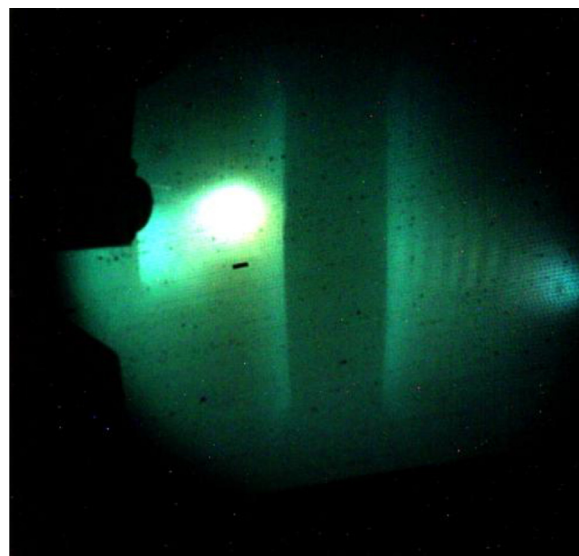


Fig. 2. Image of the Bay B electrode glow (center left) during He-GDC. The rectangular pumping duct is revealed to the left of the electrode as a region of enhanced emission due to sheath ionization [7]. The vertical dark region is the center column. The green coloration is indicative of boron compounds. (For interpretation of the references to colour in this figure legend, the reader is referred to the web version of this article.)

ment line backfilled with 1100 torr He (147 kPa) that is monitored for any pressure drop. The exhaust gas is diluted with nitrogen to a boron containing residual gas concentration to ppm levels time weighted average inside the stainless steel vacuum line after the vacuum pump. There are two GDC electrodes near the midplane, (Bays B and G) that are typically operated at 550 V and 2.3 A (Bay B) and 1.8 A (Bay G). Fig. 2 shows the plasma glow surrounding the GDC electrode at Bay B. A full-bottle boronization process begins with 30 s of helium-only GDC followed by approximately 6 h of GDC with a mix of 5% dTMB and 95% helium that consumes 9 g of dTMB followed in turn by 2 h of helium-only GDC. For a nominal vessel area of 40 m² the average coverage would be ~1400 Å thick for a nominal density of 1.6 g/cm³, but as will be seen later, the coverage is not uniform. The fill time for the supply pipe is calculated to be 2 s and it takes about 20 s to replace the NSTX-U volume with dTMB, however anomalously low deposition in the lower vessel was observed for the initial ½ h. No dTMB (65 amu) is seen in the RGA spectrum of the tokamak exhaust during the GDC. However a peak corresponding to a di-methyl boron fragment (47 amu) does appear corresponding to about 1% of the supplied dTMB.

3. Deposition during boronization

The deposition was monitored by three quartz crystal microbalances (QMB) located at the vessel wall at Bay E top, Bay B midplane and Bay F bottom [14]. These each contained a quartz crystal that oscillated at a frequency close to 6 MHz; the precise frequency depended on the deposited mass and crystal temperature. For estimation of the film thickness a nominal density of 1.6 g/cm³ was assumed. A type K thermocouple was attached to each QMB crystal housing to track the temperature. Monitoring the temperature drift and associated QMB frequency changes over weekend periods without plasmas showed that the change in crystal frequency for a temperature change of 1 °C was equivalent to a deposition of 3–8 Å (depending on the crystal). In the following the layer thickness after subtraction of temperature induced frequency changes is presented unless noted otherwise.

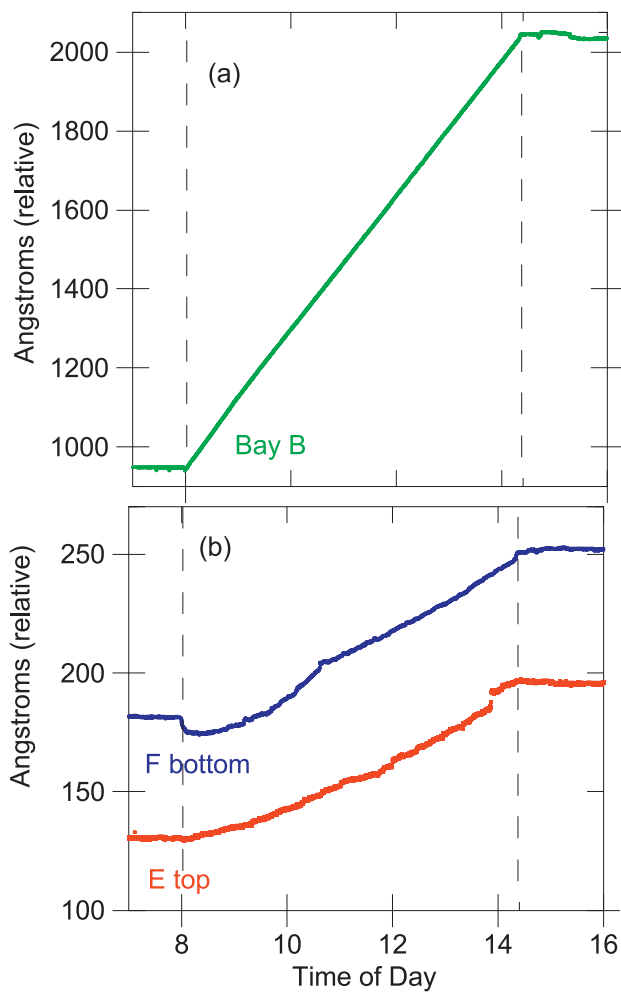


Fig. 3. Deposition at (a) Bay B midplane and (b) F bottom and E top during boronization using the Bay C lower gas injector. Note the difference in Y-axis scales.

The boronization conditions were varied in order to identify conditions of maximum deposition on the upper and lower divertors and the first experiments measured the deposition from 1.5 g dTMB at low and high pressure. Operating the glow discharge at a pressure of 2 mtorr (0.26 Pa) increased the deposition at Bay F bottom by a factor $\times 2$ – $\times 3$ and at E top by $\times 5$ – $\times 7$ compared to operation at 4 mtorr (0.53 Pa), consistent with an increased ion mean free path at the lower pressure [7]. Subsequent boronizations used 1.7 mtorr (0.23 Pa), the lowest pressure GDC could be reliably sustained. Fig. 3 shows deposition recorded at Bay B midplane, E top and F bottom during boronization using the Bay C lower gas injector and both the Bay G and Bay B GDC electrodes. It can be seen that the deposition is dominantly at the midplane (1093 Å total deposition) compared to Bay E top (66 Å) and F bottom (67 Å). Generally the ratio of B midplane deposition to F bottom and E top deposition was in the range $\times 12$ – $\times 20$, significantly more uniform than the previous range of $\times 25$ – $\times 47$. Changing the gas injection port made a minor difference. Fig. 4 shows the total deposition at the E top and F bottom QMBs from boronizations using either the F mid, D top or C lower gas injectors. It can be seen that D top injector enhances the E top deposition by 30% and the C lower injector enhances the F bottom injector by 21%. Since the lower divertor interaction is usually dominant in plasma discharges, subsequent boronizations used solely the C lower gas injector. Boronizations were also performed using only the Bay B electrode or only the Bay G electrode. The results are plotted in Fig. 5 vs. the measured

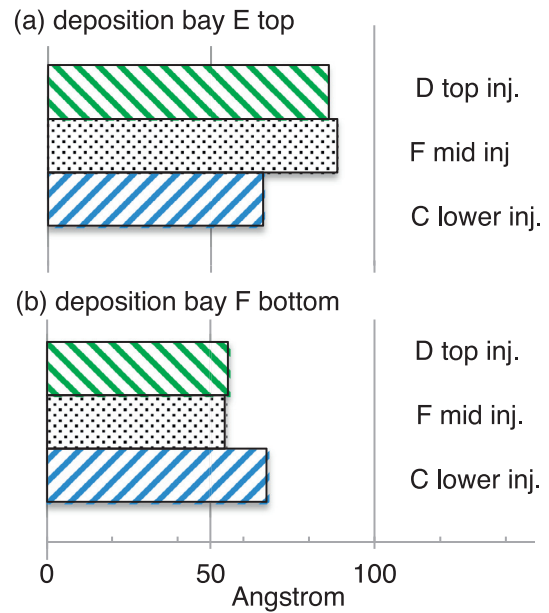


Fig. 4. The length of the bars denotes the total deposition at the E top and F bottom QMBs from boronizations using the D top, F mid, and C lower gas injectors. It can be seen that using the D top injector enhances the E top deposition by 30% and the C lower injector enhances the F bottom injector by 21%.

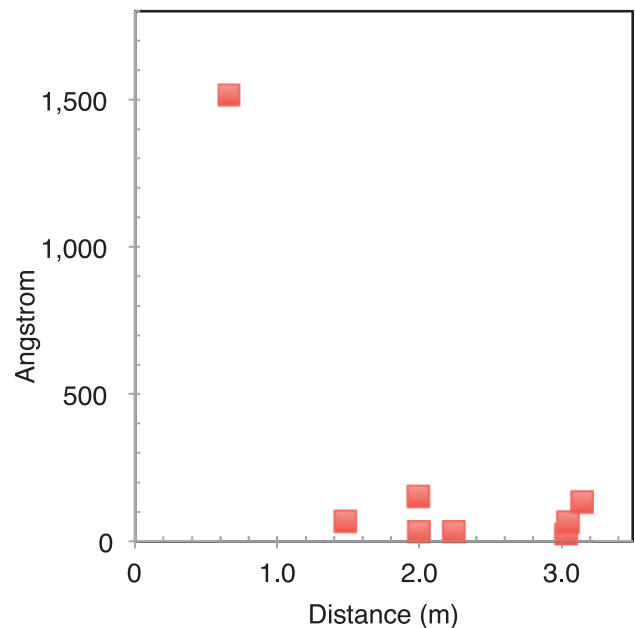


Fig. 5. Single electrode deposition on the QMBs plotted as a function of distance between the QMB and electrode in use. The high point at 1515 Å is deposition on the Bay B QMB when the nearby Bay B GD electrode is in use.

distance from the electrode in use to the QMB. The use of only one electrode changes the discharge and the sum of the deposition from using the individual electrodes separately differs from the deposition using both electrodes. Note on this day the Bay B thermocouple data acquisition had a fault, so the Bay B QMB data does not have temperature compensation – this was previously measured to be a 5% effect. A fourth QMB at Bay I midplane was operational and this data was included. In Fig. 5 the high point at 1515 Å is deposition on the Bay B QMB when the nearby Bay B GD electrode is in use (only 0.65 m away) and is consistent with the anode glow shown in Fig. 2. The deposition 2–3 m away from a GD electrode is an order-of-magnitude or more lower. It does not

follow a smooth dependence with distance, presumably because of the non-uniformity of the vacuum vessel wall (as also reported for JET in [8]).

4. Evolution of oxygen in the surface and plasma

A novel surface analysis probe, MAPP [15] was used to measure changes in surface composition of samples exposed to the boronization and to subsequent plasmas. MAPP is the first *in-vacuo* surface analysis diagnostic directly integrated into a tokamak and can perform chemical surface analysis of plasma facing samples exposed in the vessel without sample retrieval from the tokamak vacuum. On NSTX-U the MAPP is inserted into a gap at the outer perimeter of the lower divertor and the samples were inserted to a position about 4 mm above the divertor tiles (see Fig. 4 in ref. [16]). Initial X-ray photoelectron spectroscopy (XPS) measurements of the evolution of surface atomic composition of an ATJ graphite sample under boronization and subsequent plasma exposure are reported here. For these measurements the probe was retracted manually after the daily plasma operations. Remote between-discharge MAPP operation and additional capabilities for direct recoil spectroscopy, low energy ion surface spectroscopy, and thermal desorption spectroscopy will be implemented in the near future. A detailed account of NSTX-U surface chemistry changes measured by MAPP for the present period is presented in ref. [17] in this proceeding.

An ATJ graphite sample was loaded into MAPP two days before the fifth boronization, B#5. A survey XPS spectrum (800 eV–1 eV) showed 1 s spectra of carbon, boron and oxygen with no other impurities. Detailed XPS measurements of C, B, and O 1s transitions were taken on a daily basis before and after each boronization and subsequent plasma discharges with the samples remaining under the NSTX vacuum. XPS interrogates the top surface to a depth determined by the inelastic mean free path of the photo-electron. For the O 1s photoelectron energy of 674 eV the inelastic mean free path in graphite is 1.6 nm [18]. The angle between the electron analyser and sample surface is 20° so we estimate the XPS sampling depth to be $3 \times 1.6 \times \sin 20^\circ = 1.6$ nm. The surface oxygen concentration after several full-bottle boronizations using 9 g dTMB is plotted in Fig. 6(a) vs. the cumulative plasma discharge duration as defined by the plasma current exceeding $I_p = 50$ kA (typical flat-top $I_p = 600$ – 800 kA). The surface oxygen concentration measured the day after a full-bottle boronization was 4%–9% and rose up to 26% after 142 s of plasma exposure. A linear fit of B#5,7,8,9,10 data showed the O concentration increasing by 0.14% / sec of plasma from an initial value of 7.6% and is plotted as a dotted line in Fig. 6(a). During a 2-week maintenance break the surface O concentration rose from 4% after boronization#6, to 11% following venting the vessel to argon and several He-GDC tile conditioning procedures. Of course the whole period included a variety of plasma discharge conditions.

The effect of the changing surface conditions on plasma impurities was monitored by filterscopes [19] that viewed the lower divertor and observed O II 441 n.m., D- γ and D- α emission lines. The O II emission normalized to D- γ was typically lower by a factor x5 after boronization but subsequently rose back to its original value. Similar behavior was observed in the surface oxygen concentration as measured by MAPP XPS O 1s line. Both data are plotted in Fig. 6(b) vs. the normalized lower divertor D- α fluence. This pattern was consistently observed over 5 full-bottle boronizations (each 9 g-TMB). When the remote MAPP probe drive is operational we plan to correlate the full range of surface analysis data with specific plasma conditions.

Interestingly, the rise in normalized O II emission was faster after a ‘mini-boronization’ (1.5 g-TMB) as may be expected for the lower erosion lifetime of a thinner boronized layer [17]. Fig. 7

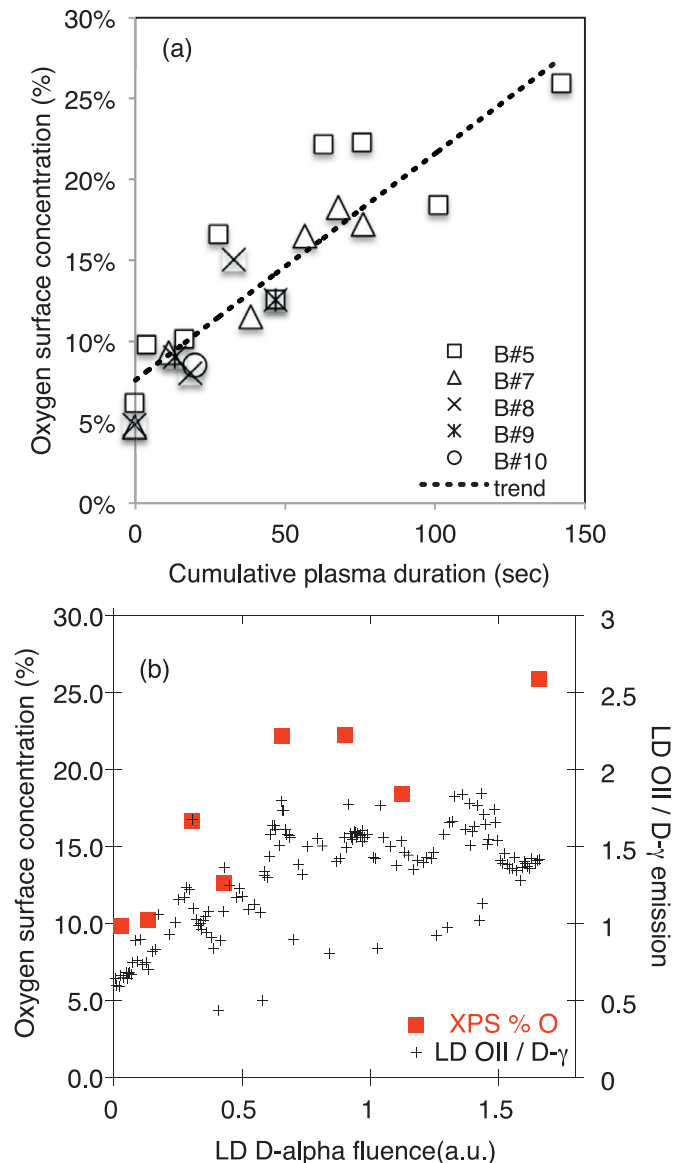


Fig. 6. (a) the evolution of surface atomic oxygen concentration as measured by MAPP XPS following full-bottle boronizations using 9 g dTMB (labelled B#5–B#10) vs. the cumulative plasma duration after each boronization, and (b) evolution of the surface atomic oxygen concentration after B#5, shown as ■, together with the ratio of O II 441 n.m. to D- γ line emission from the lower divertor, shown as +, both plotted against the cumulative lower divertor D- α fluence after B#5. The dotted line in 6 (a) is a linear fit to B#5,7,8,9,10 data.

shows the fast rise in O II emission after mini-boronization using 1.5 dTMB, compared to the slower rise after boronizations using 9 g-TMB. The fast and slow O II emission rise is consistent with the respective rise in surface atomic oxygen concentration measured by MAPP XPS providing further evidence of the correlation of plasma impurity emission and PFC surface impurity concentration.

5. Conclusions

We have characterized the deposition from new dTMB boronization system in NSTX-U. The deposition uniformity was improved by operating the glow discharge at low pressure but was still an order-of-magnitude higher in the region of the GDC electrode in the midplane than at the top and bottom divertor. The deposition could be enhanced by 20–30% by local TMB gas injection.

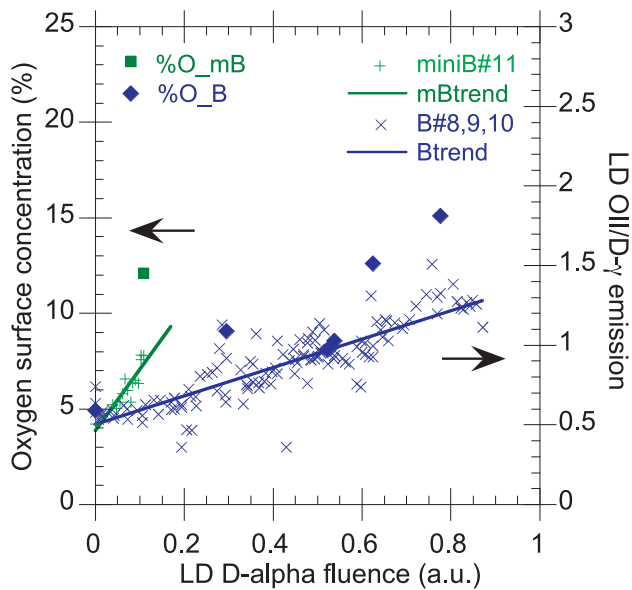


Fig. 7. Fast rise in O II emission after mini-boronization using 1.5 dTMB (shown as +, miniB#11), compared to the slower rise after full-bottle boronizations (shown as x, B#8,9,10). The fast and slow O II emission rise is consistent with the respective rise in surface atomic oxygen concentration as measured by MAPP XPS shown as ■ and ◆ respectively, all plotted against the cumulative lower divertor D- α fluence. The mBtrend and Btrend lines are linear fits to O II emission data.

One electrode was not sufficient for deposition over the whole vessel. XPS measurements of the surface oxygen concentration were made using a novel MAPP diagnostic. The fast and slow O II emission rise after mini (1.5 g-TMB) and full-bottle (9 g-TMB) boronizations was correlated with the rise in plasma facing surface atomic oxygen concentration as measured by MAPP XPS.

Acknowledgments

The authors acknowledge important contributions from R. Kaita, A. Finehart and the whole NSTX-U team. Support is provided by the U.S. DOE Contract Nos. DE AC02-09CH11466 and DE-AC52-07NA27344. The digital data for this paper can be found in <http://arks.princeton.edu/ark:/88435/dsp018s45qc26p>.

References

- [1] S. Brezinsek, et al., *J. Nucl. Mater.* 463 (2015) 11.
- [2] J. Winter, *Plasma Phys. Control Fusion* 38 (1996) 1503.
- [3] O.I. Buzhinskij, Yu.M. Semenets, *Fusion Tech.* 32 (1997) 1.
- [4] J. Winter, *J. Nucl. Mater.* 162–164 (1989) 713.
- [5] J. Winter, et al., *J. Nucl. Mater.* 176–177 (1990) 486.
- [6] C.H. Skinner, et al., *Nucl. Fusion* 42 (2002) 329.
- [7] G.J.M. Hagelaar, et al., *Plasma Phys. Control Fusion* 567 (2015) 025008.
- [8] D. Kogut, et al., *Plasma Phys. Control. Fusion* 57 (2015) 025009.
- [9] F. Ghezzi, et al., *Appl. Surf. Sci.* 354 (2015) 408.
- [10] B. Rais, PhD Thesis, Universita degli Studi di Padova, 2015.
- [11] M Ono, et al., *Nucl. Fusion* 55 (2015) 073007.
- [12] J. Menard, Overview of first operational and physics results from NSTX Upgrade, in: *Proceedings of 26th IAEA Fusion Energy Conference, Kyoto, Japan, 2016 17-22 October* submitted to *Nuclear Fusion*.
- [13] D. Cai, W. Blanchard, M. Cropper, in: *Proceedings of the Topical meeting on the Technology of Fusion Energy, Philadelphia, 2016 Aug 22-25*.
- [14] C.H. Skinner, et al., *J. Nucl. Mater.* 363-365 (2007) 247.
- [15] B. Heim, et al., *IEEE Trans. Plasma Sci.* 40 (2012) 735.
- [16] C.H. Skinner, et al., *J. Nucl. Mater.* 415 (2011) S773–S776.
- [17] F. Bedoya et al., *this issue*.
- [18] B. Lesiak, A. Jablonski, Z. Prussak, P. Mrozek, *Surf. Sci.* 223 (1989) 213.
- [19] A.L. Ramsey, S.L. Turner, *Rev. Sci. Instrum.* 58 (1987) 1211.